# Modeling electronic transport mechanisms in metal-manganite memristive interfaces

F. Gomez-Marlasca, N. Ghenzi, A. G. Leyva, C. Albornoz, D. Rubi et al.

Citation: J. Appl. Phys. **113**, 144510 (2013); doi: 10.1063/1.4800887
View online: http://dx.doi.org/10.1063/1.4800887
View Table of Contents: http://jap.aip.org/resource/1/JAPIAU/v113/i14
Published by the American Institute of Physics.

# Modeling electronic transport mechanisms in metal-manganite memristive interfaces

F. Gomez-Marlasca,[1,a)] N. Ghenzi,[1] A. G. Leyva,[1,2] C. Albornoz,[1] D. Rubi,[1,2] P. Stoliar,[1,2] and P. Levy[1,b)]
[1]*GAIyANN, Comisión Nacional de Energía Atómica-Avda. Gral Paz 1499, 1650 San Martín, Argentina*
[2]*ECyT, Universidad Nacional de San Martín, Martín de Irigoyen 3100, 1650 San Martín, Argentina*

(Received 12 March 2013; accepted 25 March 2013; published online 11 April 2013)

We studied $La_{0.325}Pr_{0.300}Ca_{0.375}MnO_3$-Ag memristive interfaces. We present a pulsing/measuring protocol capable of registering both quasi-static *i-v* data and non-volatile remnant resistance. This protocol allowed distinguishing two different electronic transport mechanisms coexisting at the memristive interface, namely space charge limited current and thermionic emission limited current. We introduce a 2-element electric model that accounts for the obtained results and allows predicting the quasi-static *i-v* relation of the interface by means of a simple function of both the applied voltage and the remnant resistance value. Each element of the electric model is associated to one of the electronic transport mechanisms found. This electric model could result useful for developing time-domain simulation models of metal-manganite memristive interfaces. © *2013 AIP Publishing LLC*. [http://dx.doi.org/10.1063/1.4800887]

## INTRODUCTION

The resistance switching (RS) effect is a reversible change in electric resistance induced by the application of voltage or current.[1] This effect is considered to play a prominent role in the next generation of nonvolatile memories.[2–4] It has been extensively studied[2–5] not only because of its technological potential and downsizeable geometry but also for mere scientific interest, as RS has been associated with memristive devices.[5,6] A RS device is classified as bipolar if the polarity of the stimulus that induces a transition from a high to a low resistance state is opposite to the one that induces a low-to-high transition. If polarity of stimuli is not relevant, RS devices are said to be unipolar.[2] According to several authors,[2–4] bipolar RS effect in metal-perovskite samples occurs at the interface and is due to an electric field driven redistribution of oxygen vacancies, near the metallic electrode, within the perovskite.

As pointed by Pickett *et al.*,[7] the lack of a time domain SPICE-like simulation model has been a major drawback for the massive adoption of bipolar RS devices in analog circuit design. In this paper, we discuss an electronic transport model that could serve as a basis for a time domain simulation model.

Several papers report the *i-v* response measurements to characterize RS phenomena in different devices.[2–5,7–11] Typical *i-v* measurements display the hysteretic response of one magnitude (*i* or *v*) respect to the other, which is injected to the RS device as a *continuous* stimulus. The presence of zero-crossing hysteresis is considered to be the fingerprint of RS effect, as the two branches of the *i-v* curve correspond to different resistance values.

The protocol presented here is based on a *pulsed* i-v measurement, as opposed to the *continuous* method. The pulsed approach is standard for electronic device testing, and is also commonly used to avoid undesired heating and/or power consumption.[12] For either a continuous or pulsed measurement, establishing the relation between nonvolatile resistance change and stimulus might be nontrivial, i.e., identifying the threshold amplitudes of nonvolatile changes might be difficult due to the smoothness of the *i-v* curve.

To gain insight into the nonvolatile resistance switch of the interface, the protocol performs an *undisturbing* measurement between every pair of pulses by injecting a reading bias so low that it does not affect the resistive state of the interface (i.e., it does not alter the oxygen vacancy distribution). The set of readings between pulses, when the pulsing sequence is cyclic, results analogous to the Hysteresis Switching Loop (HSL) introduced by Nian *et al.*[8] Thus, the protocol is capable of registering alternately both the features of a pulsed *i-v and* the features of a HSL (i.e., the relation between nonvolatile resistance and pulsing stimulus) during the same experiment. We also show a simple electronic transport model that accounts for the obtained measured data and allows predicting the quasi-static *i-v* relation of the interface by means of a simple function of both the applied voltage and the succeeding resistance value.

## EXPERIMENT DESCRIPTION

All the experiments discussed in this paper were performed at room temperature on a polycrystalline $La_{0.325}Pr_{0.300}Ca_{0.375}MnO_3$ (LPCMO) ceramic pellet with millimeter-sized Ag hand-painted contacts. Four contacts (A-B-C-D) were placed along a straight line, separated from one another by approximately 0.5 mm [see contact configuration in the inset of Fig. 1(a)]. In previous works, we discussed the non-volatile response of these devices.[11,13,14]

Current pulses were injected through contacts A and D using a Keithley 2602 SourceMeter. Recalling that bipolar RS takes place at metal-manganite interfaces exposed to

[a)]Electronic mail: marlasca@cnea.gov.ar
[b)]Electronic mail: levy@cnea.gov.ar

 

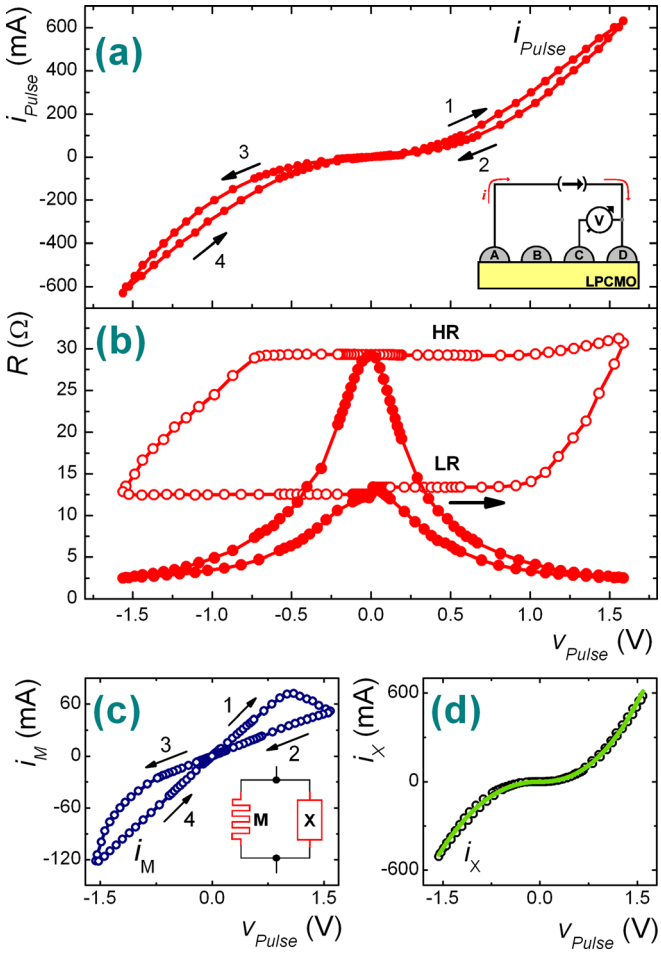


FIG. 1. (a) Dynamic $i_{Pulse}$-$v_{Pulse}$ curve obtained for the 630 mA maximum $i_{Pulse}$ amplitude loop. The arrows and numbers indicate the time evolution of the pulsing protocol. Inset: LPCMO/Ag contact configuration. (b) Open symbols: Remnant resistance measurement obtained for a 630 mA loop. The arrow indicates the time evolution of the pulsing protocol. Solid symbols: Dynamic measurement of $R_{QS}$ (defined as $v_{Pulse}/i_{Pulse}$) registered during the 630 mA loop. Notice that $R_{QS}$ tends to $R_{Rem}$ as $v_{Pulse}$ tends to 0 (or, more precisely, as $i_{Pulse}$ tends to $I_{Bias}$) both for the HR and LR states. (c) $i_M$ values obtained for the 630 mA loop. Inset: Electric model for the LPCMO/Ag interface. (d) Open circles: $i_X$ values obtained by computing $i_X = i_{Pulse} - i_M$ for every ($i_{Pulse}$, $i_M$) value pair. Solid line: Curve obtained by fitting $i_X = \alpha \cdot |v_{Pulse}|^{\beta}$ to the calculated $i_X$ data set. Parameters $\alpha$ and $\beta$ are polarity dependant, see text.

some electric stimulus, then contacts A and D were interfaces that experienced *complementary* RS.[11] In this paper, we will focus on a single active interface (namely, the interface D), as results for the other contact are equivalent, except for reversed pulsing polarity.

Since bulk resistance (defined as $V_{BC}/I_{AD}$, $I_{AD}$ small[15]) remained approximately constant at 35 mΩ, and resistance between terminals C and D (defined as $R_{CD} = V_{CD}/I_{AD}$) varied between 10 and 40 Ω, then voltage drop between contacts C and D was mainly due to contact D, i.e., the one that endured current passage. For this reason, we will refer to quantities like $v_{CD}$, $R_{CD}$, etc., simply as $v$, $R$, etc., all of them related to contact D.

The measuring protocol comprised a sequence of two alternated measurements: the pulsed *i-v* (or *dynamic* measurement) and the undisturbing measurement between pulses (*remnant* measurement). The *dynamic* measurement was performed by applying a series of short current pulses $i_{Pulse}$ through contacts A and D, while voltage drop $v_{Pulse}$ was measured between contacts C and D, using the sense terminals of the Keithley 2602 SourceMeter as a voltmeter. These pulses lasted about 1 ms each, and their amplitudes were sequenced to sweep in arbitrary steps from 0 to a maximum current value, then from the maximum to the minimum, and finally from the minimum back to 0, so as to complete a cycle. The pulses were square-shaped, except for short transients at the edges. As $v_{Pulse}$ was measured during the flat part of the pulses, the registered $v_{Pulse}$ values are considered to be quasi-static values.[16]

To avoid local heating and to allow the intermediate undisturbing measurement, time elapsed between pulses was kept longer than 2 s. The *remnant* measurement consisted in applying a small bias current $I_{Bias}$ in between pulses so as to measure the remnant resistance of the interface D (defined as $R_{Rem} = V_{Bias}/I_{Bias}$) without affecting it in an irreversible way. The undisturbing value chosen for $I_{Bias}$ was 300 μA.[15]

## INTERFACE CHARACTERIZATION

The solid-circle line in Fig. 1(a) corresponds to the pulsed $i_{Pulse}$-$v_{Pulse}$ curve obtained during a pulsing sequence cycle with maximum current amplitude of ±630 mA. Notice that it exhibits both hysteretic and nonlinear behavior. Being a smooth response, the onset of irreversibility is difficult to assign. The open-circle curve in Fig. 1(b) shows results obtained from the remnant measurement displayed as a function of $v_{Pulse}$, i.e., the voltage drop measured while injecting $i_{Pulse}$ that preceded each remnant measurement. Notice that the remnant resistance cycle describes a loop that exhibits two well-defined plateaus, corresponding to a High remnant (HR) and a Low remnant (LR) resistance states. The steep remnant resistance transition between them is attributed to changes in the oxygen vacancy profile of the interface that happens when the electric stimulus is high enough to overcome the anchoring energy of the atoms to the matrix.

By defining the *quasi-static resistance* (i.e., the resistance measured while pulsing) as $R_{QS} = v_{Pulse}/i_{Pulse}$, the $i_{Pulse}$-$v_{Pulse}$ measurement shown in Fig. 1(a) can also be displayed as the solid-circle curve in Fig. 1(b). Note that, as expected, $R_{QS}$ tends to $R_{Rem}$ as $v_{Pulse}$ tends to 0 (or, more precisely, as $i_{Pulse}$ tends to $I_{Bias}$) both for HR and LR states. Nonetheless, as the amplitude of $v_{Pulse}$ increases from ~0 V, $R_{QS}$ and $R_{Rem}$ become more and more dissimilar.

Let us consider the LR state in Fig. 1(b). As $v_{Pulse}$ departs from 0 V, no remnant resistance change occurs until $v_{Pulse}$ surpasses a threshold of approximately 1 V. On the other hand, $R_{QS}$ decreases monotonically as the amplitude of $v_{Pulse}$ increases. Since no noticeable remnant resistance change occurs for $v_{Pulse} < 1$ V, then no change of vacancy distribution is expected to explain the $R_{QS}$ reduction observed as $v_{Pulse}$ increases. Thus, it is clear that a reversible, nonlinear electronic transport mechanism must account for the difference between $R_{Rem}$ and $R_{QS}$.

With the aim of studying the small-current range where $R_{Rem}$ and $R_{QS}$ start diverging, we performed a series of experiments whose results are displayed in Fig. 2. This figure

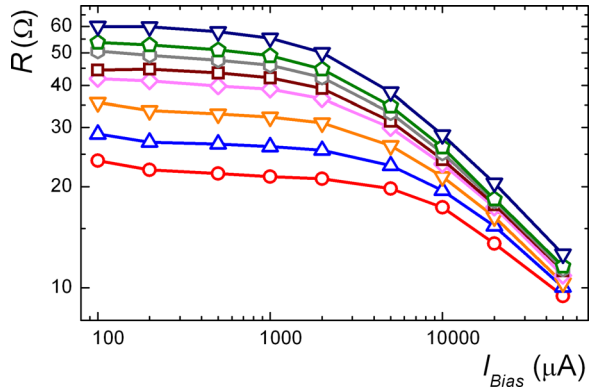


FIG. 2. Eight different remnant resistance states measured with increasing $I_{Bias}$. Notice that all the remnant resistance states remain almost constant (i.e., the interface presents linear *i-v*) between 100 $\mu$A and 1 mA. As $I_{Bias}$ increases, though, the remnant resistance measurements decrease, which implies the *i-v* relation is no longer linear.

shows eight measurements of different remnant resistance states at interface D, plotted against increasing $I_{Bias}$. Each remnant resistance state was obtained by applying a pulsing/measuring sequence similar to that previously described, except that the pulsing sequence was stopped when the desired (arbitrary) remnant resistance value was attained. Each remnant resistance state was then measured with increasing $I_{Bias}$ values, none of them large enough to induce a RS transition. Notice that the remnant resistance value of each state remained almost constant within the 100 $\mu$A-1 mA $I_{Bias}$ range. Nonetheless, as $I_{Bias}$ was further increased, resistance measurement values started decreasing noticeably. It is worth mentioning that the value chosen for $I_{Bias}$ when acquiring the results displayed in Fig. 1(b) ($I_{Bias} = 300\ \mu$A) was well below the nonlinear threshold.

The response of the interface to increasing bias current may be qualitatively described as a resistance $R_{Rem}$ in parallel to a non-linear device (NLD) that resembles a couple of antiparallel diodes. Let us discuss the response of such a NLD. First recall that a diode's resistance is extremely large when reverse voltage is applied, decreases monotonically when forward voltage increases, and tends to some extremely large value when forward voltage tends to 0. Thus, a couple of antiparallel diodes will behave as a NLD that exhibits a monotonic decreasing resistance $R_{NLD}$ for increasing voltage amplitude (regardless of the polarity) or an extremely large resistance $R_{NLD}$ when voltage tends to 0. Therefore, when a small current $I_{Bias}$ is injected, a small voltage develops at the interface. If this voltage is sufficiently small, then the NLD will exhibit a resistance $R_{NLD}$ much larger than $R_{Rem}$. Thus, the total parallel resistance, defined as $(R_{Rem}{}^{-1} + R_{NLD}{}^{-1})^{-1}$, must amount to approximately $R_{Rem}$. On the other hand, as $I_{Bias}$ increases, voltage increases too, leading $R_{NLD}$ to decrease accordingly. Hence, the total parallel resistance must decrease as $I_{Bias}$ increases, which qualitatively explains the results displayed in Fig. 2. Recall these results were obtained for very small currents, i.e., for currents not high enough to induce resistance switching.

Consider again the results shown in Fig. 1(a). As previously remarked, this dynamic $i_{Pulse}$-$v_{Pulse}$ curve displays both hysteretic behavior (i.e., resistive switching) and nonlinear electronic transport. We will now discuss a model that accounts quantitatively for these results, which is a generalization of the model we used to describe the results displayed in Fig. 2. We propose to model the direct-current response of the interface with the two-element electric circuit shown in the inset of Fig. 1(c). The element $M$ represents a linear electronic transport memristive device we will associate with $R_{Rem}$. The element $X$, on the other hand, represents a NLD whose dependence on $v_{Pulse}$ and vacancy distribution is yet to be determined. Therefore, $i_{Pulse}$ is considered to be split into two: the current that flows through $M$, which we define as

$$i_M = v_{Pulse}/R_{Rem} \tag{1}$$

and the current that flows through $X$, defined as $i_X = i_{Pulse} - i_M$. Recall that $R_{Rem}$ is measured *after* each pulse by injecting $I_{Bias}$, and $v_{Pulse}$ is measured *while* injecting $i_{Pulse}$; thus, calculating $i_M$ and $i_X$ requires data both from remnant and dynamic measurements. Fig. 1(c) shows the results obtained for $i_M$ and Fig. 1(d) shows the results obtained for $i_X$ (open circles). The $i_M$ curve describes a highly hysteretic zero crossing loop along its cycle. Notice that the resistance value of $M$ was point by point defined to be that of $R_{Rem}$ [see Eq. (1)]; therefore, $R_{Rem}$ is considered to be the resistive manifestation of the memristive device $M$. Two segments of the $i_M$-$v_{Pulse}$ cycle exhibit linear *i-v* response, corresponding to HR and LR levels in Fig. 1(b). Remarkably, the obtained $i_M$ curve is qualitatively similar to that simulated by Strukov *et al.*[5] for a linear *i-v*, bipolar, voltage-driven nonlinear ionic drift memristor. The $i_X$ values were obtained by simply subtracting the $i_M$ curve from the $i_{Pulse}$ curve.

The obtained $i_X$ curve presents two noticeable features. First, it seems to be almost non-hysteretic when compared to the curves obtained for $i_{Pulse}$ and $i_M$, that is to say, $X$ appears to be much less susceptible than $M$ to the mechanism behind RS. Second, the $i_X$-$v_{Pulse}$ relation of $X$ does resemble the *i-v* relation of a couple of antiparallel diodes, in the sense that almost no current flows through it when $v_{Pulse}$ is small [consider the plateau centered about $v_{Pulse} = 0$ V in Fig. 1(d)] but becomes more and more conductive as the amplitude of $v_{Pulse}$ increases. This explains the convergence of $R_{QS}$ and $R_{Rem}$ as voltage tends to 0 [see Fig. 1(b)] and their divergence as the amplitude of $v_{Pulse}$ increases.

We can gain some insight of the transport mechanism of the element $X$ by fitting the $i_X$-$v_{Pulse}$ data. It was found that the function that fits best the $i_X$-$v_{Pulse}$ data was the power law $i_X(v_{Pulse}) = \alpha \cdot |v_{Pulse}|^{\beta}$, with $\alpha \approx 0.212$ ($\alpha \approx -0.184$) and $\beta \approx 2.21$ ($\beta \approx 2.29$) for $v_{Pulse}$ positive (negative). Notice that the parameters $\alpha(\beta)$ obtained for both polarities are very similar. This function is also displayed in Fig. 1(d) as a solid line. As the Space Charge Limited Current (SCLC) transport mechanism has a square law $i \propto v^2$ correlation,[17] it appears to be the mechanism behind $X$. The small difference from 2 of the obtained $\beta$ values may be due to other slighter nonlinear effects. According to Tsui *et al.*,[17] who also studied electronic conduction in ceramic manganite samples, different mechanisms seem to outstand at different voltage regimes. Namely, thermionic emission limited conduction (TELC)

seems to be prominent at the small voltage regime (where this mechanism presents linear *i-v* correlation) and SCLC seems to outstand at higher voltages, where a square law dependence emerges. This is remarkably consistent with the two-element parallel model: *M* (linear by definition) is prominent at lower voltages and *X* (which exhibits a nearly square law dependence) gains importance as $v_{Pulse}$ increases. Hence, each element of the model is thought to stand for a different electronic transport mechanism: the linear element *M* stands for TELC conduction and *X* represents SCLC conduction.

## USING THE ELECTRONIC TRANSPORT MODEL

In order to check the consistency of this 2-element model as a way to account for the quasi-static *i-v* response of Ag-LPCMO interfaces, we will compare experimental data with calculations done by applying the model. Before doing so, the mathematical implications of the model will be discussed.

Accounting for the quasi-static behavior of the interface means inferring either $i_{Pulse}$ or $v_{Pulse}$ from the other quantity and the values of the circuit elements. Since the proposed model is a 2-element parallel circuit, the simplest choice is calculating $i_{Pulse}$ from $v_{Pulse}$, as voltage is the common parameter to all elements of a parallel circuit. Mathematically, the model states that the current $i_{Pulse}$ that flows through the interface is the sum of the currents that circulate through the discrete elements *X* and *M*, each of them standing for a different electronic transport mechanism. Therefore,

$$i_{Pulse}(v_{Pulse}, \boldsymbol{w}) = i_X(v_{Pulse}, \boldsymbol{w}) + i_M(v_{Pulse}, \boldsymbol{w}), \quad (2)$$

where $\boldsymbol{w}$ represents a vector that accounts for the vacancy distribution near the interface and $i_X$ and $i_M$ are the currents that flow through each of them. We will now restrict the analysis to the case in which *X* is non-hysteretic, a situation we will associate with small changes in the oxygen vacancy distribution near the interface. Recall that, in our experiments, the $i_X$-$v_{Pulse}$ relation obtained for the 630 mA cycle [Fig. 1(d)] exhibited nearly non-hysteretic behavior. It will be assumed that the $i_X$-$v_{Pulse}$ relation of *X* is the one we found, i.e., $i_X(v_{Pulse}) = \alpha \cdot |v_{Pulse}|^{\beta}$, being $\alpha$ and $\beta$ polarity dependant. Stating also that the $i_M$ dependence on $v_{Pulse}$ is that of Eq. (1), we can now rewrite Eq. (2) as,

$$i_{Pulse}(v_{Pulse}, \boldsymbol{w}) = \alpha \cdot |v_{Pulse}|^{\beta} + v_{Pulse}/R_{Rem}(\boldsymbol{w}). \quad (3)$$

Thus, if *X* is assumed to be non-hysteretic, then $R_{Rem}$ (i.e., *M*) is the only quantity that depends explicitly on the vacancy distribution $\boldsymbol{w}$. Notice that Eq. (3) allows calculating the current $i_{Pulse}$ of each pulse by replacing in it the parameters $\alpha$ and $\beta$, the voltage $v_{Pulse}$ applied to the interface *while* pulsing, and the remnant resistance of the interface $R_{Rem}$ *after* pulsing.[16] As calculating the value of $i_{Pulse}$ of a given pulse requires knowing the remnant resistance $R_{Rem}$ of the interface after applying it, the value of $R_{Rem}$ has to be known beforehand. The model described by Rozenberg *et al.*[14] could be used for predicting $R_{Rem}$, as it relates remnant resistance switching with vacancy distribution and its dynamics.

We will now discuss a series of additional RS experiments in which we compare registered $i_{Pulse}$ values with their corresponding calculated values, obtained by using Eq. (3). Note that, as they were available, *measured* $R_{Rem}$ values were used in the equation, so there was no need for predicting $R_{Rem}$. Also recall that the experimental setup actually injects current pulses, but both $i_{Pulse}$ and $v_{Pulse}$ values are registered while pulsing. Thus, the model will be checked by "predicting" the injected $i_{Pulse}$ values from the measured $v_{Pulse}$ values.[18]

Fig. 3(a) shows an experiment performed on the same contact D as before. It is the dynamic measurement obtained during a 600 mA maximum amplitude cycle loop (solid pentagons) and the corresponding remnant resistance measurement, displayed as the open pentagons' line. The open circles are the calculated $i_{Pulse}$ current values. These values were obtained by replacing the measured $R_{Rem}$ values and using the same $\alpha$ and $\beta$ parameters obtained for the 630 mA loop data set. As shown in Fig. 3(a), registered and calculated values appear to be remarkably similar: calculation errors range from 1% to 15% with respect to the registered values, with an average error below 6%.

A "random write" pulsing experiment was also performed in the same contact. Fig. 3(b) shows an arbitrary $i_{Pulse}$ pulsing sequence as a function of time (solid tilted squares) and the corresponding calculated $i_{Pulse}$ values (open

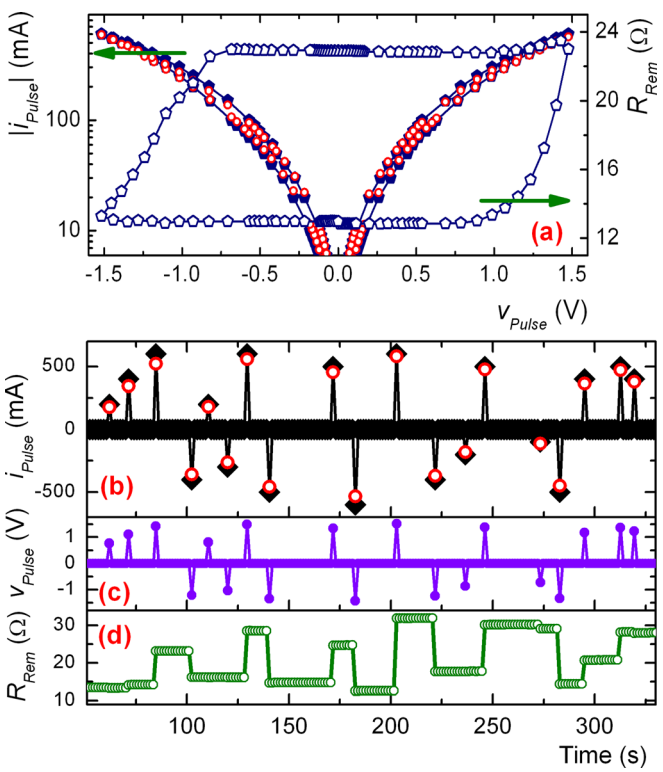


FIG. 3. (a) Solid pentagons: $i_{Pulse}$-$v_{Pulse}$ curve measured during a 600 mA maximum $i_{Pulse}$ amplitude loop. Open pentagons: Remnant measurement corresponding to the 600 mA loop. Open circles: Calculated $i_{Pulse}$-$v_{Pulse}$ values. (b) Solid tilted squares: Arbitrary $i_{Pulse}$ sequence plotted against time. Open circles: Calculated $i_{Pulse}$ intensities, obtained by using the measured $v_{Pulse}$ intensities (c) and the measured remnant resistance $R_{Rem}$ (d).

circles). The $i_{Pulse}$ values were calculated by using the same $\alpha$ and $\beta$ parameters as before, the measured $R_{Rem}$ values displayed in Fig. 3(d) and the $v_{Pulse}$ values displayed in Fig. 3(c). The calculation error now lies in the 3%−15% range, with an average error of 9%.

It should be noted that other sets of experiments were performed in this and other similar interfaces, and it was always possible to find a range of current amplitudes in which the element *X* presented almost non-hysteretic response, compared with that of element *M*. However, when the limits of this current amplitude range were surpassed, the hysteretic $i_X$-$v_{Pulse}$ response of *X* did start to become noticeable.

## CONCLUSIONS

We presented a protocol that allowed measuring both dynamic and remnant aspects of a nonlinear electronic transport memristive interface. It proved to be a suitable tool for linking the pulsed *i-v* response of the interface to its remnant resistance state. A two-component electric model was proposed to account for the obtained results, which shed light on the nature of the coexisting electronic transport mechanisms of the interface, namely TELC and SCLC. The mechanisms found are consistent with those formerly described by Tsui *et al.*[17] The electric model also allowed decoupling (to some extent) the vacancy diffusion problem from the electronic transport mechanisms. By assuming that $R_{Rem}$ is the resistance value of a linear electronic transport memristive device *M* (as the one previously simulated by Strukov *et al.*[5]), it was possible to isolate the nonlinear transport mechanism and associate it with a nonlinear element *X*. The idea of a diode-like NLD in parallel with a memristive device was previously suggested[9] (as an *ad hoc* model) to account for dynamic experimental results. The possibility of acquiring both dynamic and remnant experimental data effectively allowed isolating and studying the nonlinear mechanism. Surprisingly, it was found that *X* exhibits nearly non-hysteretic behavior within a certain range, as opposed to its linear counterpart *M*. This fact allowed calculating $i_{Pulse}$ from the values of $v_{Pulse}$ and $R_{Rem}$ within that range (i.e., where the vacancy distribution changes were said to be small) via Eq. (3).

Both the measuring protocol and the electric model could result useful for characterizing other memristive-interface memory cells. Measuring dynamic and remnant features is necessary for estimating critical parameters like power consumption during write time, $\Delta R_{Rem}$ versus applied stimulus, etc. The proposed 2-component model could be used to extend the simulation model of Rozenberg *et al.* (which accounts only for remnant resistive switching) to predict dynamic behavior as well. Since this simulation model associates remnant resistance switching to voltage-driven vacancy redistribution, the quasi-static value of $i_{Pulse}$ could be calculated if both the $v_{Pulse}$ value used in each simulation step and the $R_{Rem}$ value obtained after it are replaced in a properly adjusted version of Eq. (3). This approach could lead to a useful time domain SPICE-like model for these memristive interfaces.

## ACKNOWLEDGMENTS

We would like to thank Dr. F. Palumbo for his valuable assistance. We acknowledge support from CONICET PIP 0047 "MeMO" and DuPont-CONICET 2010 "MeMOSat." D.R. and P.L. are members of CONICET.

[1]A. Kingon, Nature Mater. **5**, 251–252 (2006).
[2]A. Sawa, Mater. Today **11**, 28 (2008).
[3]R. Waser, R. Dittmann, G. Staikov, and K. Szot, Adv. Mater. **21**, 2632–2663 (2009).
[4]D. S. Jeong, R. Thomas, R. S. Katiyar, J. F. Scott, H. Kohlstedt, A. Petraru, and C. S. Hwang, Rep. Prog. Phys. **75**, 076502 (2012).
[5]D. B. Strukov, G. S. Snider, D. R. Stewart, and R. S. Williams, Nature **453**, 80–83 (2008).
[6]L. Chua, Appl. Phys. A **102**, 765–783 (2011).
[7]M. D. Pickett, D. B. Strukov, J. L. Borghetti, J. J. Yang, G. S. Snider, D. R. Stewart, and R. S. Williams, J. Appl. Phys. **106**, 074508 (2009).
[8]Y. B. Nian, J. Strozier, N. J. Wu, X. Chen, and A. Ignatiev, Phys. Rev. Lett. **98**, 146403 (2007).
[9]J. J. Yang, M. D. Pickett, X. Li, D. A. A. Ohlberg, D. R. Stewart, and R. S. Williams, Nat. Nanotechnol. **3**, 429 (2008).
[10]A. Sawa, T. Fujii, M. Kawasaki, and Y. Tokura, Jpn. J. Appl. Phys. **44**, L1241–L1243 (2005).
[11]M. Quintero, P. Levy, A. G. Leyva, and M. J. Rozenberg, Phys. Rev. Lett. **98**, 116601 (2007).
[12]B. Fisher, J. Genossar, L. Patlagan, and G. M. Reisner, Appl. Phys. Lett. **95**, 132501 (2009).
[13]N. Ghenzi, M. J. Sánchez, F. Gomez-Marlasca, P. Levy, and M. J. Rozenberg, J. Appl. Phys. **107**, 093719 (2010).
[14]M. J. Rozenberg, M. J. Sánchez, R. Weht, C. Acha, F. Gomez-Marlasca, and P. Levy, Phys. Rev. B **81**, 115101 (2010).
[15]As explained below and shown in Fig. 2, $I_{Bias} = I_{AD} = 300\,\mu$A ensures that $R_{Rem}$ is measured within its linear response regime, without affecting irreversibly the state of the interface.
[16]See supplementary material at http://dx.doi.org/10.1063/1.4800887 for details on pulse voltage profile measurements and a discussion about which remnant resistance value is considered, i.e., the one measured after pulsing or the one measured before.
[17]S. Tsui, A. Baikalov, J. Cmaidalka, Y. Y. Sun, Y. Q. Wang, Y. Y. Xue, C. W. Chu, L. Chen, and A. J. Jacobson, Appl. Phys. Lett. **85**, 317 (2004).
[18]Current pulses were chosen instead of voltage pulses because the Ag-LPCMO samples had two RS-active interfaces in series, hence controlling the voltage applied to one of them only would have required a much more intricate (and slow) closed-loop pulsing/measuring system.